frontiers in Microbiology

ORIGINAL RESEARCH
published: 08 September 2020
doi: 10.3389/fmicb.2020.572631

Establishment of a Replicon Reporter of the Emerging Tick-Borne Bourbon Virus and Use It for Evaluation of Antivirals

*Siyuan Hao[1], Kang Ning[1], Xiaomei Wang[1], Jianke Wang[1], Fang Cheng[1], Safder S. Ganaie[1], John E. Tavis[2] and Jianming Qiu[1]**

[1] Department of Microbiology, Molecular Genetics and Immunology, University of Kansas Medical Center, Kansas City, KS, United States, [2] Department of Molecular Microbiology and Immunology, Saint Louis University, St. Louis, MO, United States

Bourbon virus (BRBV) was first isolated from a patient hospitalized at the University of Kansas Hospital in 2014. Since then, several deaths have been reported to be caused by BRBV infection in the Midwest and Southern United States. BRBV is a tick-borne virus that is widely carried by lone star ticks. It belongs to genus *Thogotovirus* of the *Orthomyxoviridae* family. Currently, there are no treatments or vaccines available for BRBV or thogotovirus infection caused diseases. In this study, we reconstituted a replicon reporter system, composed of plasmids expressing the RNA-dependent RNA polymerase (RdRP) complex (PA, PB1, and PB2), nucleocapsid (NP) protein, and a reporter gene flanked by the 3′ and 5′ untranslated region (UTR) of the envelope glycoprotein (GP) genome segment. By using the luciferase reporter, we screened a few small molecule compounds of anti-endonuclease that inhibited the nicking activity by parvovirus B19 (B19V) NS1, as well as FDA-approved drugs targeting the RdRP of influenza virus. Our results demonstrated that myricetin, an anti-B19V NS1 nicking inhibitor, efficiently inhibited the RdRP activity of BRBV and virus replication. The IC_{50} and EC_{50} of myricetin are 2.22 and 4.6 μM, respectively, in cells. Myricetin had minimal cytotoxicity in cells, and therefore the therapeutic index of the compound is high. In conclusion, the BRBV replicon system is a useful tool to study viral RNA replication and to develop antivirals, and myricetin may hold promise in treatment of BRBV infected patients.

Keywords: tick-borne virus, thogotovirus, Bourbon virus, RNA-dependent RNA polymerase, replicon reporter, antivirals

OPEN ACCESS

Edited by:
Jianrong Li,
The Ohio State University, United States

Reviewed by:
Wenjun Ma,
University of Missouri, United States
Zhilong Yang,
Kansas State University, United States

****Correspondence:***
Jianming Qiu
jqiu@kumc.edu

Specialty section:
This article was submitted to Virology, a section of the journal Frontiers in Microbiology

Received: *15 June 2020*
Accepted: *21 August 2020*
Published: *08 September 2020*

Citation:
Hao S, Ning K, Wang X, Wang J, Cheng F, Ganaie SS, Tavis JE and Qiu J (2020) Establishment of a Replicon Reporter of the Emerging Tick-Borne Bourbon Virus and Use It for Evaluation of Antivirals. Front. Microbiol. 11:572631. doi: 10.3389/fmicb.2020.572631

INTRODUCTION

Bourbon virus (BRBV) is a member in the genus *Thogotovirus* of the *Orthomyxoviridae* family. There are seven genera in the family of *Orthomyxoviridae*, which are segmented negative-strand RNA viruses (Kawaoka and Palese, 2006), including four types of influenza viruses (influenza virus A, B, C, and D), thogotovirus, quaranjavirus, and isavirus. Many viruses in the *Orthomyxoviridae* family are important pathogens to humans or animals. The epidemic/pandemic influenza A viruses have caused millions of human deaths in the past century and are still circulating, posing a huge

threat to human health and the economy. Thogotoviruses mainly circulate in domestic animals, such as sheep, cattle, and camels, causing neural diseases and abortion. Two thogotoviruses, thogoto virus, and dhori virus, have been reported to infect humans and cause deaths (Butenko et al., 1987; Kosoy et al., 2015). Human antibodies against thogoto virus and dhori virus have been detected in Europe, Asia, and Africa (Filipe et al., 1985; Hubalek and Rudolf, 2012). It has been reported that thogoto virus can cause human infections in a vector-free manner, possibly by an aerosol route (Butenko et al., 1987), highlighting the potential to infect humans in a large population.

Bourbon virus was first isolated from a blood sample of a hospitalized male patient from Bourbon County, Kansas, United States, in the spring of 2014 at the University of Kansas Hospital (Kosoy et al., 2015). The patient died due to a complex syndrome of leukopenia, lymphopenia, thrombocytopenia, hyponatremia, and increased levels of aspartate aminotransferase and alanine aminotransferase. Due to the high level of viremia and unique identification of the virus in the serum taken from the patient, BRBV was believed to be the cause of the illness and the death of the patient. Later, two additional cases of BRBV infection have been reported. In 2015, a patient from Payne County, Oklahoma, United States tested positive for neutralization antibodies to BRBV before fully recovering (Savage et al., 2017). In June 2017, a 58-year-old woman from Missouri died from an infection of BRBV after she had been misdiagnosed for a significant period of time (Bricker et al., 2019). Not surprisingly, a high seroprevalence of BRBV-neutralizing antibodies in raccoons (50%) and white-tailed deer (86%) was detected in MO, United States (Jackson et al., 2019). However, the Center for Disease Control and Prevention (CDC), United States, currently does not know if the virus may be found in other areas of the United States, since a seroprevalence of BRBV infection has not been evaluated outside of these epidemic regions. Nevertheless, BRBV is the first species of the genus *Thogotovirus* of the *Orthomyxoviridae* family to be identified as a human pathogen in the New World (Lambert et al., 2015).

Bourbon virus is widely carried by the lone star tick (*Amblyomma americanum*), a species that is aggressive, feeds on humans, and is widely distributed across the East, Southeast, and Midwest States. BRBV was found in three pools of lone star ticks from retrospective tests in 39,096 ticks from northwestern Missouri, 240 km from Bourbon County, Kansas, United States (Savage et al., 2017). The human BRBV and the strain isolated from tick pools share >99.0% sequence at the amino acid level and 95.0% identity at the RNA sequence level (Savage et al., 2017). BRBV replicates in cell lines derived from the hard ticks *Amblyomma*, *Hyalomma*, and *Rhipicephalus* (Lambert et al., 2015). Together with the geographic location of the BRBV infection and the geographic distribution of a number of *A. americanum* ticks (Savage et al., 2017, 2018), these studies strongly suggest that the lone star tick is a vector of BRBV transmission to humans.

Little is known about the biology of BRBV. Due to the high mortality of BRBV infection, specific treatments with antiviral drugs are in demand to save lives. In this study, we established a replicon reporter of BRBV. We then used the replicon reporter to examine anti-influenza drugs that target viral RNA-dependent RNA polymerase (RdRP) and endonuclease inhibitors of human parvovirus B19 (B19V) for inhibition of BRBV RdRP activity and BRBV replication in HEK293T and Vero cells.

MATERIALS AND METHODS

Cells and Virus

Cell Cultures

HEK293T cells (ATCC CRL-11268) and Vero cells (ATCC CCL-81, gifted from Dr. Maria Kalamvoki) were cultured in Dulbecco's modified Eagle's medium (DMEM) (HyClone, catalog no. SH30022.01; GE Healthcare Life Sciences, Logan, UT, United States) supplemented with 10% fetal bovine serum (FBS) (catalog no. F0926, Sigma, St. Louis, MO, United States) at 37°C under a 5% CO_2 atmosphere.

Virus

BRBV-KS (#NR-50132) was obtained through BEI Resources, NIAID, NIH. The virus was amplified on Vero cells once, aliquoted, and stored at −80°C in the Hemenway 4037 biology safety level 3 (BSL3) Lab of the University of Kansas Medical

TABLE 1 | Primers and probe used in the study.

Target	Name	5′-3′
PA	FPApcDNA-*Hin*dIII	AGA TCT AAG CTT AGC AAA AAC AAG CAG TAA TTG
	RPApcDNA-*Xho*I	AGA GTC CTC GAG AGA GAA ATC AAA GCA GTT TTT TC
PB1	FPB1pcDNA-*Bam*HI	AGA TCT GGA TCC AGC AAA AAC AAG CAG TTG TTA ACC
	RPB1pcDNA-*Xho*I	AGA GTC CTC GAG AGA GAA ATC AAA GCA GTT TTT TC
PB2	FPB2pcDNA-*Hin*dIII	AGA TCT AAG CTT AGC AAA AAC AAG CAG TTA TTC GAC
	RPB2pcDNA-*Xho*I	AGA GTC CTC GAG AGA GAA ATC AAA GCA GTT TTT TC
NP	FNPpcDNA-*Hin*dIII	AGA CTC AAG CTT AGC AAC AAC AAG CAG TTG TTC
	RNPpcDNA-*Xho*I	AGA GTC CTC GAG AGA GAA ATC AAA GCA GTT TTT TC
GP	FGPpcDNA-*Hin*dIII	CTG TAC AAG CTT AGC AAA AAC AAG CAG ATT GTC CAA AGA TGA ATG CCC T
	RGPpcDNA-*Xho*I	AGA GTC CTC GAG AGA GAA ATC AAA GCA GTT TTT TC
	FGPpHW	TGG GGG GGA GGA GAC GAG CAA AAA CAA GCA G
	RGPpHW	CCG GGT TAT TGG AGA CGA GAG AAA TCA AAG CAG TTT TTT
M	FMpcDNA-*Nde*I	GCA TCA CAT ATG GCT CAC CAG GTT GCA GCA GG
	RMpcDNA-*Xho*I	GTC ACT CTC GAG TTC GAC ACT CTT CAG GAG TTG GTA C
qPCR	FqPCR-NP	GCA AGA AGA GGC CAG ATT TC
	RqPCR-NP	TCG AAT TCA GCA TTC AGA GC
	NP PROBE	6-FAM/CCT CAC ACC/ZEN/ACG GAA GCT GGG-ABkFQ

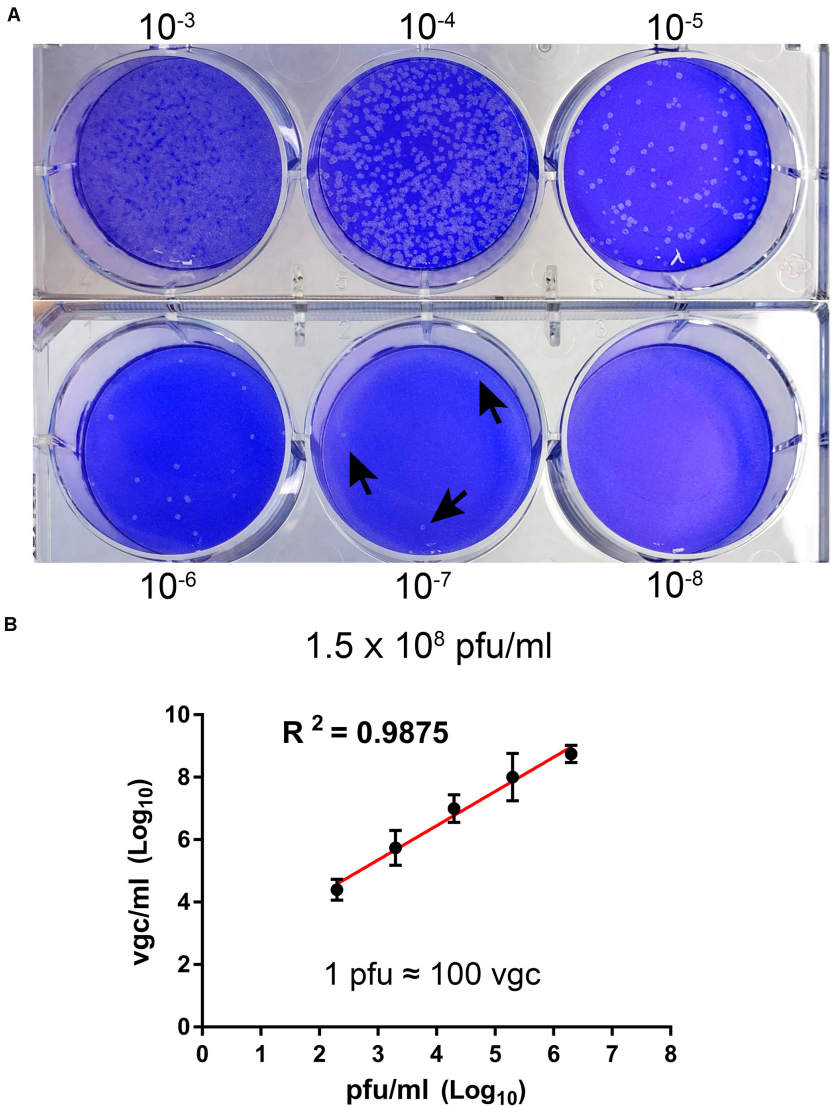

FIGURE 1 | Titration of BRBV stock. **(A)** Plaque assay. Vero cell monolayers on a six-well plate were infected with 200 μl of serial 10-fold diluted BRBV-KS as indicated. Plaques were visualized by staining with crystal violet after 5 days of infection on Vero cells. Arrows indicate plaques. **(B)** Comparison between plaque assay and RT-qPCR. The same virus stock was diluted by serial 10-fold dilution. RT-qPCR was used to quantify the vgc number. The linear regression has a R^2 of 0.9875, indicating 1 plaque forming unit (pfu) equals ∼100 vgc. The data presented are averages and standard deviations from three independent experiments, with each experiment analyzing samples in duplicate.

Center and used for all subsequent studies. A biosafety protocol to work on the virus in the BSL3 Lab was approved by the Institutional Biosafety Committee (IBC) of the University of Kansas Medical Center.

Compounds

T705 (Favipiravir) and VX-787 were purchased from AdooQ Bioscience (Irvine, CA, United States). Baloxavir (S-033447; Baloxavir acid) was purchased from MedChemExpress (Monmouth Junction, NJ, United States). Flavonoid compounds used in this study were commercially acquired as follows: #7 (Idofine #2030), #9 (Sigma, #70050), #135 (AldrichSelect #361173301), #201 (Sigma, #S0327), #860 (Enamine, #Z1918018629). They all had a purity of ≥95%. All compounds were dissolved in DMSO (Sigma, St. Louis, MO, United States) as stock solutions at 10 mM, and stored at −80°C.

Virus Titration Assays

Plaque Assays

Cells were seeded in six-well plates at a density of 2×10^6 cells and were confluent the following day. We used the cell growth media to serially dilute the virus stock at 10-fold. 200 μl of the diluent were added to each well and incubated for 1 h with gently rocking the plate every 20 min.

After removing the virus diluent, 2 ml of overlay media, 1% methylcellulose (Sigma, M0387) in DMEM with 5% FBS, were added to each well. The plates were incubated at 37°C under 5% CO_2 for 5 days. After removing the methylcellulose overlays, cells were fixed using the 10% formaldehyde solution for at least 30 min and stained with 1% crystal violet solution.

Reverse Transcription and Quantitative PCR (RT-qPCR)

Viral RNA was isolated from virus preparation or supernatants of virus-infected cells using a viral RNA extraction kit (Quick-RNA Viral Kit, R1035, Zymo Research) by following the manufacturer's instructions. M-MLV reverse transcriptase (#M368A, Promega) was used to reverse transcribe viral RNA with the reverse PCR primer according to the manufacturer's instructions. Then, the transcribed cDNA was subjected to qPCR using primers and a TaqMan probe targeting to the nucleocapsid (NP) gene of BRBV (**Table 1**) with a 7500 Fast Real-Time PCR System (Applied Biosystems). In order to eliminate the contamination of free viral RNA, we quantified the nuclease digestion-resistant viral genome copies (vgc) numbers. To this end, 100 μl of virus preparations were treated with 25 units of Benzonase (Sigma) for 30 min before RNA isolation.

Viral cDNA Cloning and Plasmid Constructions

pcDNA3-Based Viral cDNA Plasmids

Bourbon virus RNA was isolated from a stock of BRBV-KS passaged on Vero cells. cDNA of each viral RNA genome fragment was synthesized using the reverse primer and amplified by PCR. The amplification program started with one cycle at 48°C for 45 min and one cycle at 94°C for 2 min. These cycles were followed by 40 cycles at 94°C for 20 s, 52°C for 30 s, and 72°C for 40 s; the program ended with one cycle at 72°C for 5 min. The PCR products were visualized by agarose gel electrophoresis, extracted, and cloned into pcDNA3 vector (Invitrogen), resulting in pcDNA-(BRBV) PA, PB1, PB2, M, NP, and glycoprotein (GP) plasmids.

pHW2000-GP Plasmid

The plasmid pHW2000 (Hoffmann et al., 2002) contains the human ribosome RNA polymerase I (pol I) promoter and the murine terminator sequence separated by two *Bsm*BI sites. The pol I promoter and terminator elements are flanked by a truncated immediate-early promoter of cytomegalovirus (CMV) and by the bovine growth hormone polyadenylation signal (bGHpA). The pcDNA3-GP was used as a template to amplify the GP cDNA with a primer set that has the *Bsm*BI sites (**Table 1**). After digestion of the PCR products with *Bsm*BI, the fragments were cloned into the pHW2000 vector, which resulted in the pHW2000-(BRBV)GP plasmid.

Reporter Plasmids

pHW-ΔCMV-GP was constructed by deletion of the CMV promoter in pHW2000-GP. Then, we constructed pHW-ΔCMV-GP-GFP and pHW-ΔCMV-GP-gLuc plasmids inserting the GFP open reading frame (ORF) through the *Nde*I and *Eag*I sites of the GP ORF and replacing the GP ORF with the *Gaussia luciferase* (*gLuc*) ORF, respectively, into the pHW-ΔCMV-GP plasmid (**Figure 4A**).

The sequences of all the primers are listed in **Table 1**. All the constructed plasmids were sequenced to confirm the cloned cDNA sequences at MCLAB (South San Francisco, CA, United States). DNA sequence analyses were performed using SnapGene 4.0 (SnapGene, Chicago, IL, United States).

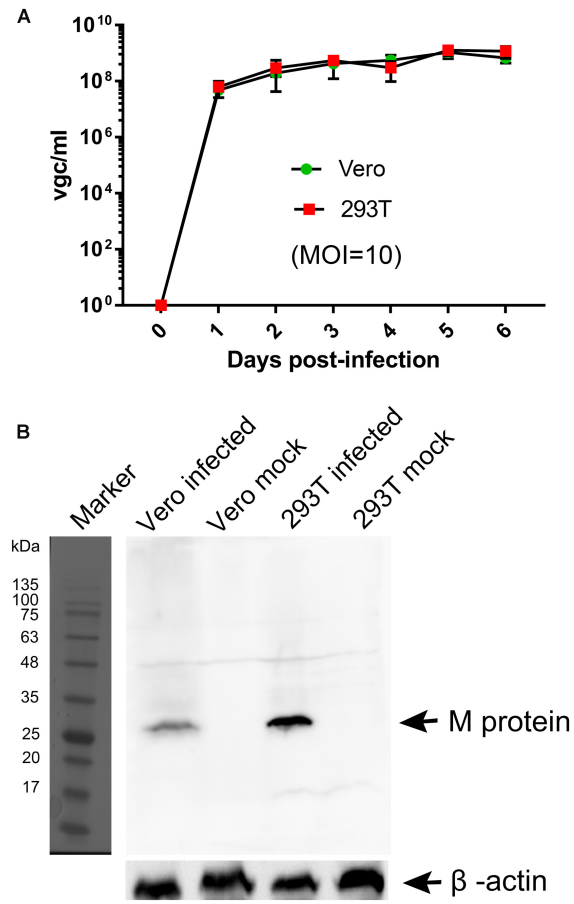

FIGURE 2 | Comparisons of BRBV-KS infection between Vero and HEK293T cells. **(A)** BRBV growth kinetics. Cells were infected with BRBV-KS at an MOI = 10 pfu/cell. Cell culture media (supernatants) were collected daily for 6 days. Viral RNA was extracted from the samples of supernatants and then titrated by a RT-qPCR assay. The data present the means with standard deviations, which are obtained from three independent experiments, with each experiment analyzing samples in duplicate. **(B)** Western blotting. ~5 × 10^4 infected cells were lyzed in 1 × Laemmli sample buffer and loaded in SDS-10% polyacrylamide gel for separation. The gel was transferred to a polyvinylidene difluoride membrane, which was blotted with an anti-BRBV M protein rat polyclonal antibody. The M protein in BRBV-infected Vero and HEK293T cells was detected at ~30 kDa as indicated, but not in mock-infected cells. β-actin was probed as a loading control. Original images can be found in "**Supplementary Material**".

A

Segment	Nucleotide sequences
NP-(KP657749)	222-AACTTTGTGTTTGAG-236
NP-(Cloned)	222-CT··A·TGTGA··GC-236
M-(KU708254)	749-T-749
M-(Cloned)	749-C-749
PB1-(KP657750)	1741-TGCAGCGGAACGA-1755
PB1-(Cloned)	1741-A···TATC···TC-1755

B

Protein	Identity	Amino acids
PB1	99.4%	C573S S574I G575S I577L
NP	98.9%	T67S L68I C69V L70M S71A

FIGURE 3 | Sequence variations of the cloned BRBV genome segments. **(A)** Nucleotide sequence variations. Nucleotide changes in BRBV-KS in comparison to the sequences of BRBV genome segments deposited in Genbank. **(B)** Amino acid sequence variations. Percent identity at the amino acid level and amino acid alternations of the PB1 and NP proteins between sequences of BRBV-KS and the ones deposited in GenBank. No variations were found in PA, PB2, and GP proteins.

Plasmid DNA Transfection

HEK293T cells were transfected using the PEImax (Cat# 24765-2, MW 40,000, Polysciences, Inc.) at a ratio of 1:3 of DNA: PEI in 200 μl of opti-MEM (Invitrogen) (Wang et al., 2018). The total amounts of plasmid DNA were kept constant (2–3 μg per well of six-well plate) in each group by supplementation with an empty vector.

BRBV Reporter Assays

BRBV GFP Reporter Assay

pHW-ΔCMV-GP-GFP was co-transfected with the four pcDNA-PA, PB1, PB2, and NP plasmids into HEK293T cells confluent in six-well plates. After 7 days post-transfection, the GFP signal was observed under a fluorescent microscope (Nikon Ti-S). The transfection of pHW-ΔCMV-GP-GFP with three pcDNA plasmids (PB1, PB2, NP) was set as a negative control.

BRBV Luciferase Reporter Assay

pHW-ΔCMV-GP-gLuc and the four pcDNA-based plasmids were co-transfected into HEK293T cells in 96-well plate. At 3 days post-transfection, 10 μl of the cell culture supernatants were taken and mixed with 50 μl of Working solution or luciferase activity, using the *gLuc* Flash Assay kit (Pierce™, #16159). Luminescent signals were detected on a Synergy H1 microplate reader (BioTek, Winooski, VT, United States). Three pcDNA plasmids (PB1, PB2, and NP) and pHW-ΔCMV-GP-gLuc co-transfected cells were set up as a negative control.

Half Cytotoxic Concentration (CC_{50}) Assay

The cytotoxicity of compounds on HEK293T and Vero cells was evaluated using the CytoTox-Glo™ Cytotoxicity Assay kit (Promega, #G9290), according to the manufacturer's instructions. Cells were seeded at 4×10^4 cells per well in 96-well plates. After overnight incubation, different concentrations of the compounds diluted in culture media were added to each well. Cells treated with DMSO were used for the negative control. Cell viability was measured after 3 days of incubation.

Half Maximal Effective Concentration (EC_{50}) Assay

Confluent monolayers of Vero and HEK293T cells in 96-well plates were inoculated with 10 pfu of BRBV. Different concentrations of the compounds, diluted in medium, were added to the wells. Each concentration of the compounds was tested in duplicate per experiment, and the experiment was repeated three times. At 3 days post-infection, culture supernatants were collected and used to quantify the nuclease digestion-resistant vgc numbers using reverse transcription and quantitative PCR (RT-qPCR).

Western Blotting

Cells were collected by centrifugation and lysed using a 1 ml tuberculin syringes. The cell lysates were loaded, along with 2.5 μl of a pre-stained protein ladder (#P008; GoldBio,

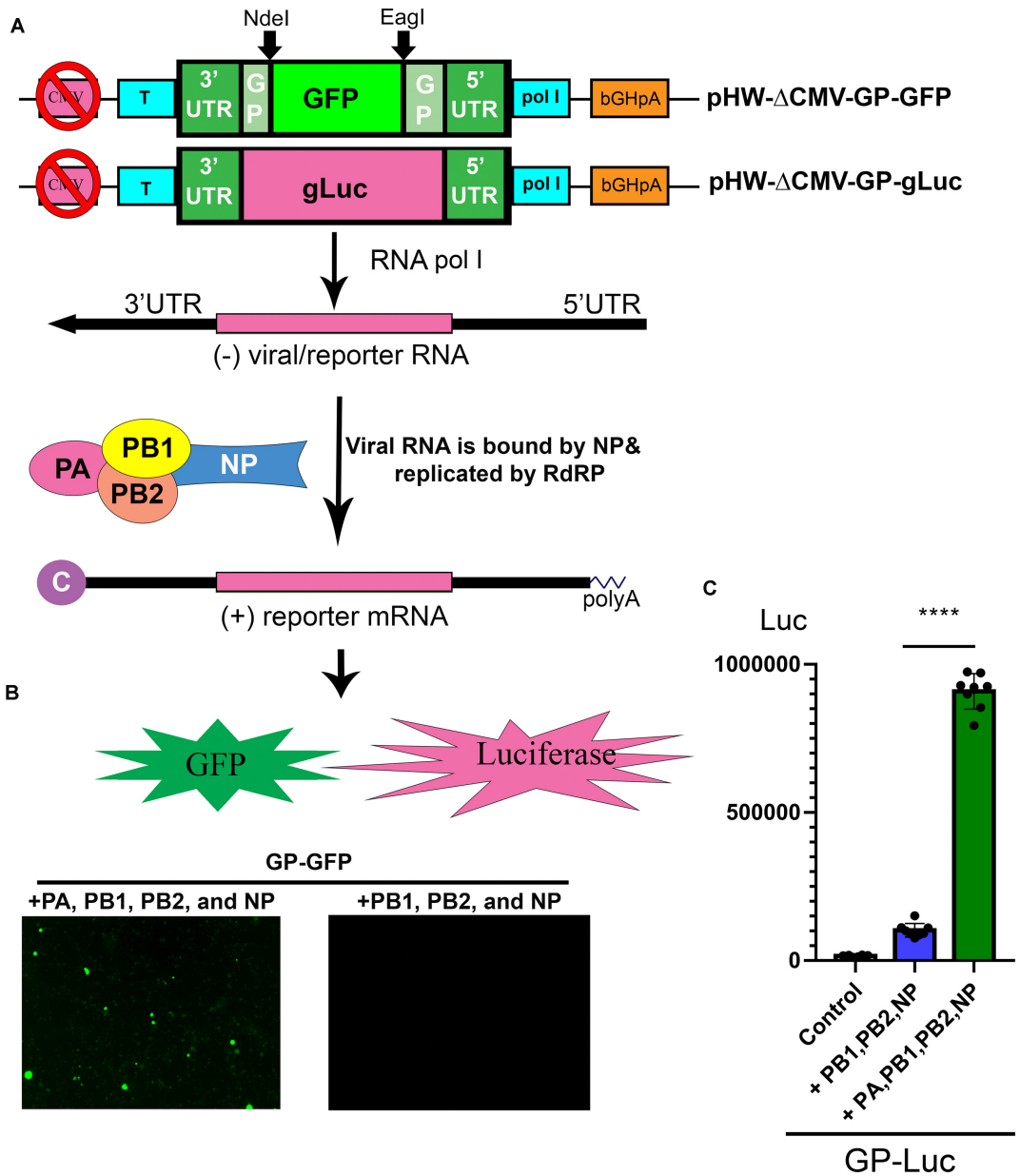

FIGURE 4 | Establishment of a BRBV replicon report system. **(A)** Diagram of the reporter system. In a CMV pol II-deleted pHW-ΔCMV-GP plasmid, a GFP open read frame (ORF) or a *gLuc* ORF was inserted into the pol I expression cassette to obtain pHW-ΔCMV-GP-GFP and pHW-ΔCMV-GP-gLuc. In cells transfected with pcDNA-PA, PB1, PB2, and NP plasmids, pol I transcribes negative sense viral (reporter) RNA [(-)rRNA], which is used as a template for replication of (-)rRNA and production of reporter mRNA (GP-GFP or GP-gLuc) by the RdRP complex and NP protein as diagrammed. Then reporter mRNA is translated to express GFP or gLuc. Since the CMV pol II promoter was removed, the production of reporter mRNA is solely dependent on the replication of the reporter RNA (the activity of the RdRP complex). "C" at the 5′ end of the (+) reporter mRNA represents the 5′ m7G cap. **(B)** Expression of PA, PB1, PB2, and NP supported GFP expression from the GP-GFP gene. Co-transfection of the pHW-ΔCMV-GP-GFP with pcDNA-PA, PB1, PB2, and NP in HEK293T cells revealed green fluorescence under a UV microscope, but the co-transfection with only pcDNA-PB1, PB2, and NP did not. **(C)** PA, PB1, PB2, and NP expression supported gLuc expression from GP-gLuc gene. Co-transfection of the pHW-ΔCMV-GP-gLuc with pcDNA-PA, PB1, PB2, and NP in HEK293T cells showed a high luciferase activity (green bar), but not with only three pcDNA plasmids or no plasmids (control). All luciferase activities (Luc) were detected by the *Gaussia* Luciferase Glow Assay Kit (Pierce). Individual values are represented by black solid dots and the columns are the means with standard deviations from eight experiments performed in duplicate. ****$P < 0.0001$ by one-way Student *t*-test.

St. Louis, MO, United States), and separated on a 10% SDS-polyacrylamide gel. Proteins were transferred onto a polyvinylidene difluoride membrane (#IPVH00010; Millipore, Bedford, MA, United States). The membrane was blocked and probed with primary and secondary antibodies sequentially. Signals were visualized by enhanced chemiluminescence, and

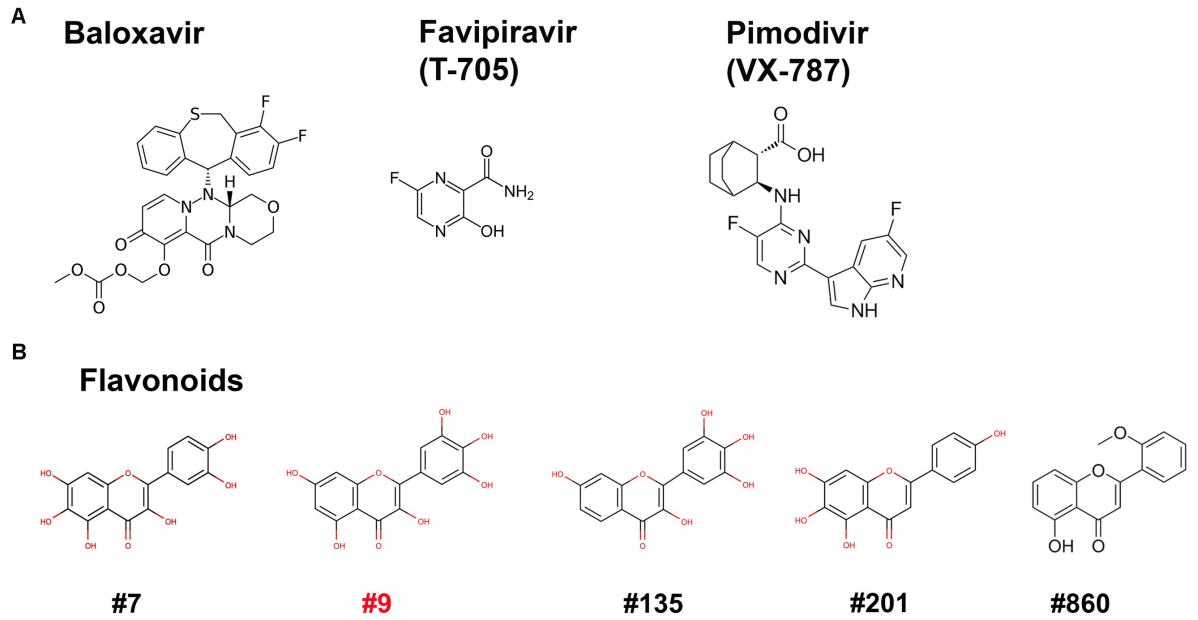

FIGURE 5 | Compound structures. Structures of the three inhibitors of anti-RdRP of influenza **(A)** and 5 flavonoids **(B)** are shown.

the pre-stained protein ladder was imaged under bright light simultaneously under a Fuji LAS 4000 imaging system.

An anti-BRBV M protein polyclonal antibody was produced in rats by immunizing them with the BRBV M protein, which was expressed and purified in bacteria, following a protocol previously described (Sun et al., 2009). Anti-β-actin (#A5441) antibody was purchased from Sigma (St. Louis, MO, United States).

Statistical Analysis

Inhibitory concentration (IC_{50}), cytotoxic concentrations (CC_{50}), and Effective Concentration (EC_{50}) were determined with the means and standard deviations obtained from three independent experiments performed in duplicate. Calculations of IC_{50}, CC_{50}, and EC_{50} and statistical analysis were done by using GraphPad Prism version 8.0. Error bars represent means and standard deviations (SD), and statistical significance (*P* value) was determined by using 1-way ANOVA analysis, followed by Tukey-Kramer post-test for comparison of three or more groups and unpaired (Student) *t*-test for comparison of two groups.

RESULTS

BRBV-KS Infection of HEK293T Cells

We propagated BRBV-KS, obtained from BEI Resources[1], in Vero cells. At 7 days post-infection, when most of the cells appeared cytopathic, the media were collected and centrifugated. The supernatant was collected, aliquoted, and stored at −80°C. The virus was titrated on Vero cells with a titer of 1.5×10^8 plaque forming units (pfu)/ml (**Figure 1A**). We next developed a RT-qPCR to quantify the vgc numbers in the BRBV stock. We found a high correlation of the vgc numbers with the pfu titrated ($R^2 = 0.9875$) (**Figure 1B**). In the following experiments, we used the RT-qPCR to quantify the virus.

We tested human HEK293T cells for infection of BRBV for comparison with infection in Vero cells. Virus growth was determined over the course of infection, and infected cells were collected at 6 days post-infection for Western blotting of matrix (M) protein expression. The results showed that BRBV infected HEK293T cells displayed similar growth kinetics as those in Vero cells (**Figure 2A**), which had a peak of virus production of approximately (∼) 10^9 vgc/ml in the media, as well as detection of the M protein at a size of ∼30 kDa (**Figure 2B**).

Cloning of the BRBV cDNA Fragments

To clone the 6 cDNAs of the 6 genome segments of BRBV-KS, we designed primers complementary to the 3′ and 5′ untranslated region (UTR) of the originally published genome sequences of BRBV-KS, KU708255 (*GP*), KU708254 (*PB1*), KU708253 (*PB2*), KP657749 (*NP*), KP657750 (*M*), and KP657748 (PA) (**Table 1**). Each viral gene was reversely transcribed using each forward primer and PCR amplified using respective paired primers (**Table 1**). The PCR cDNA fragments were first cloned into pcDNA3 and sequenced. Sequences of *GP*, *PA*, and *PB2* genes were confirmed as identical to those originally deposited in GenBank; whereas *NP*, *PB1*, and *M* genes have 10, 7, and 1 nucleotide variations, respectively (**Figure 3A**), which result in amino acid variations in NP and PB1 (**Figure 3B**).

We next used the set of pHW primers (**Table 1**) that had the *Bsm*BI sites to amplify the GP cDNA and cloned it in a *Bsm*BI-digested pHW2000 bidirectional cloning vector (Hoffmann et al.,

[1]www.beiresources.org/

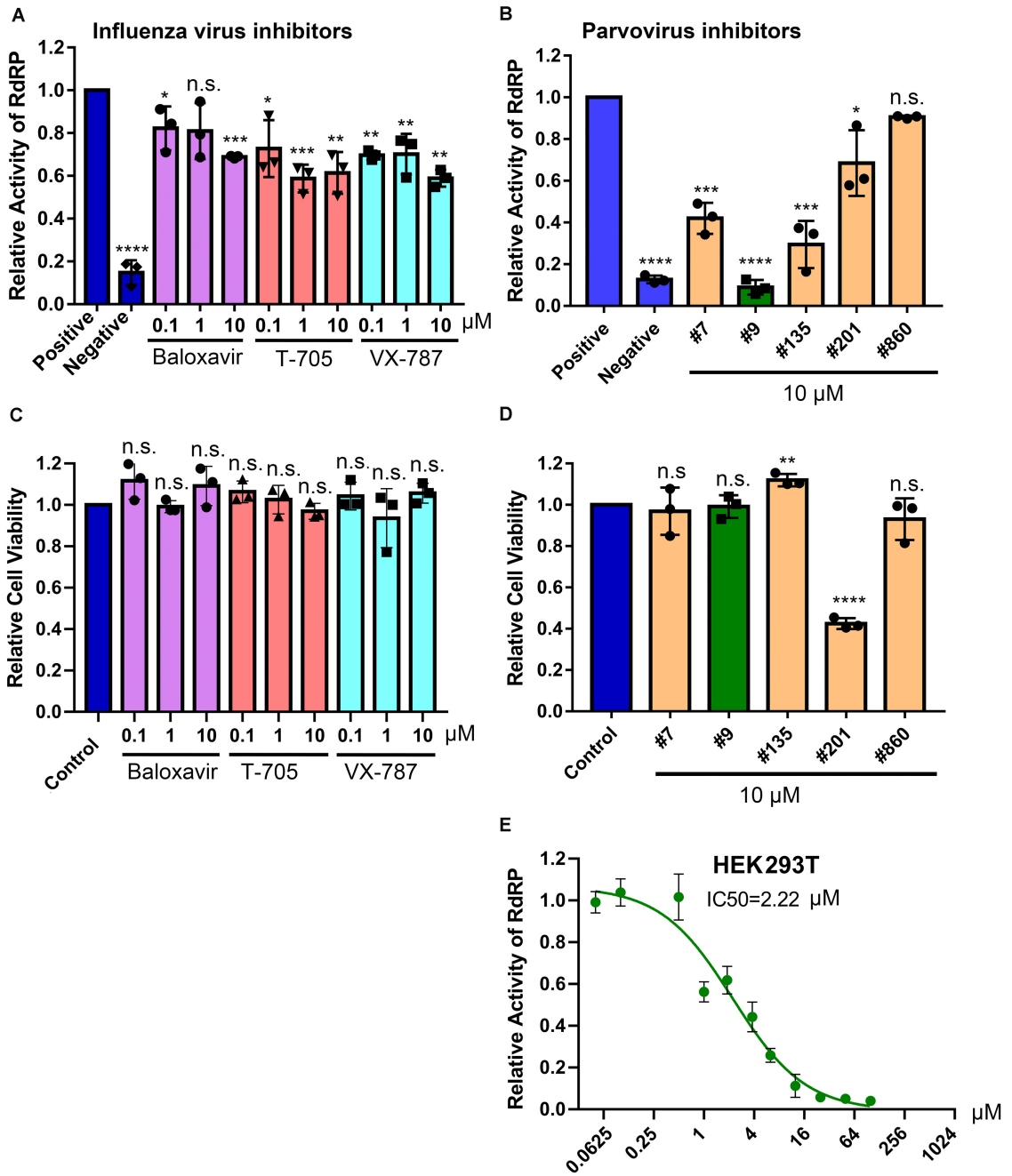

FIGURE 6 | Screening of BRBV RdRP inhibitors using the BRBV replicon luciferase reporter. **(A,B)** Inhibition of RdRP activity. The inhibitory effect of different drugs, inhibitors targeting RdRP of influenza virus (Flu inhibitors) **(A)** and inhibitors of anti-parvovirus endonuclease compounds (Parvovirus inhibitors) **(B)**, on BRBV RdRP activity was quantified using the GP-gLuc reporter assay at different concentrations as indicated. DMSO was used as a positive control of the reporter (Positive), and transfection with only pcDNA-PB1, PB2, and NP was used as a negative control of the reporter (Negative). At 3 days post-transfection, the activity of the expressed *Gaussia* luciferase was quantified using a *Gaussia* Luciferase Glow Assay Kit (Pierce). Results from each compound were normalized to the vehicle control in each experiment and were expressed with the means and standard deviations obtained from three experiments performed in duplicate. **(C,D)** Cytotoxicity assay. Compounds were assayed for cytotoxicity in HEK293T cells at the concentrations indicated using a CytoTox-Glo™ Cytotoxicity Assay kit (Promega). The results are normalized to the mock-treated control (set as 1.0). Values are the means and standard deviations obtained from three experiments, each performed in duplicate. **(E)** IC_{50} of compound #9 on RdRP activity. Compound #9 was applied to HEK293T cells transfected with the gLuc reporter system of five plasmids at various concentrations as indicated. The polymerase activity was quantified by measuring the luciferase activity. Values are the means with standard deviations and are normalized to the mock group from three experiments performed in duplicate. The half maximal inhibitory concentration (IC_{50}) was calculated with GraphPad Prism software. *P* values are calculated using one-way and Tukey–Kramer post-test, compared with DMSO or mock control. $^{*}P < 0.05$; $^{**}P < 0.01$; $^{***}P < 0.001$; $^{****}P < 0.0001$; and n.s. ($P > 0.05$) denotes no statistical significance.

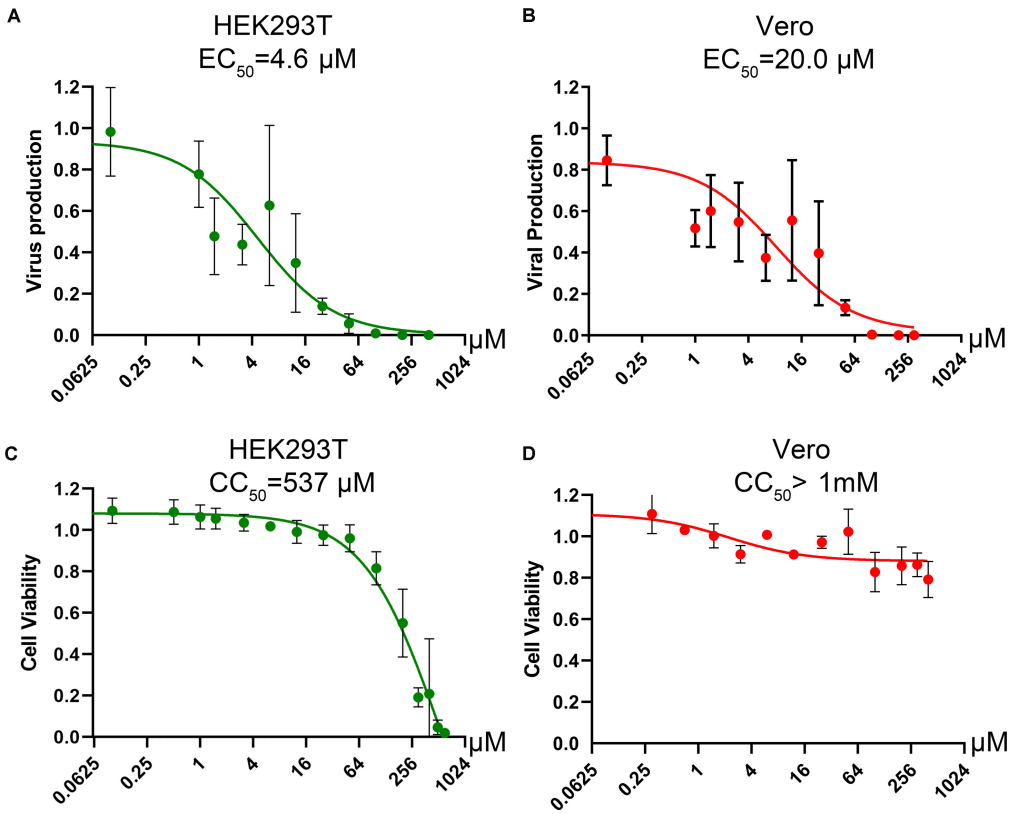

FIGURE 7 | Determination of the CC_{50} and EC_{50} of compound #9 in cell cultures. **(A,B)** EC_{50} of compound #9. HEK293T cells **(A)** or Vero cells **(B)** were infected with BRBV at an MOI of 10, followed by application of compound #9 at various concentrations as indicated. At 3 days post-treatment, RT-qPCR was performed to quantify the vgc numbers in the cell culture media. Values are the means with standard deviation and are normalized to a mock group, and were obtained from three experiments, each performed in duplicate. The EC_{50} was calculated using GraphPad Prism software. **(C,D)** CC_{50} of compound #9. A cytotoxicity assay was used to measure the viability of HEK293T cells **(C)** or Vero cells **(D)** affected by compound #9 at various concentrations as indicated. The percentage of viable cells were determined using a CytoTox-Glo cytotoxicity assay kit (Promega). The results are shown as relative values to the mock control cells. Values are the means with standard deviation obtained from three experiments performed in duplicate. The CC_{50} was calculated using GraphPad Prism software.

2002). The pHW2000-GP clone that had the right direction of BRBV cDNAs was confirmed by sequencing, in which there is the immediate early promoter of CMV, RNA polymerase II (pol II) promoter, a pol I terminator in the 3′ UTR, a ribosome RNA pol I promoter and a bGHpA in the 5′ UTR.

Establishment of a Viral RNA Dependent RNA Polymerase (RdRP) Activity Assay, a Replicon Reporter System of BRBV

Working on BRBV requires a BSL3 facility, thus, a replicon system of BRBV is important for assessing antivirals in a BSL2 setting and for high throughput screening of antivirals. Based on the pHW-ΔCMV-GP plasmid, we inserted a GFP ORF and a secreted *gLuc* ORF between the 3′ and 5′ UTR of the GP segment (**Figure 4A**), which resulted in plasmids pHW-ΔCMV-GP-GFP and pHW-ΔCMV-gLuc. When pHW-ΔCMV-GP-GFP was co-transfected with pcDNA-PA, PB1, PB2, and NP plasmids in HEK293T cells, at 7 days post-transfection, green fluorescence was clearly observed in cells transfected with pcDNA-PA, PB1, PB2, and NP plasmids but not in cells transfected with all plasmids except pcDNA-PA (**Figure 4B**). Similarly, a high luciferase activity was detected in the cells co-transfected with pHW-ΔCMV-GP-gLuc and pcDNA-PA, PB1, PB2, and NP plasmids, but nearly background levels were detected in cells transfected with pHW-ΔCMV-GP-gLuc and pcDNA-PB1, PB2, and NP plasmids (**Figure 4C**). Overall, there was a 10-fold increase in luciferase activity by the addition of the pcDNA-PA plasmid, suggesting a function of the RdRP activity from expression of PA, PB1, PB2, and NP.

Compound #9, a Natural Flavonoid Myricetin, Effectively, Inhibits BRBV RdRP Activity and BRBV Replication in Cells

We next used the BRBV replicon reporter system to test antiviral activity of three inhibitors of influenza virus RdRP, favipiravir, also known as T-705 (a pan RdRP inhibitor) (Furuta et al., 2005; Fuchs et al., 2019), pimodivir (VX-787), an inhibitor of PB2 cap-snatching activity (Byrn et al., 2015; Furuta et al., 2017), and baloxavir, a PA endonuclease inhibitor (Omoto et al., 2018)

(**Figure 5A**). At 0.1, 1 and 10 μM, respectively, none inhibited luciferase (RdRP) activity by >50% (**Figure 6A**). These drugs did not exhibit significant cytotoxicity at the tested concentrations in HEK293T cells (**Figure 6C**).

Since influenza virus PA exerts endonuclease activity on both single-stranded (ss)RNA and ssDNA (Doan et al., 1999; Klumpp et al., 2000; Dias et al., 2009), we tested four flavonoid compounds (#7, #9, #135, and #201) (**Figure 5B**) that inhibit nicking/endonuclease activity of the large non-structural protein (NS1) of B19V on an ssDNA template (Xu et al., 2018). Surprisingly, at 10 μM, 3 flavonoids (#7, #9, and #135) inhibited BRBV RdRP activity by >50%. In contrast, flavonoids #201 and #860 did not inhibit RdRP (**Figure 6B**). Additional evidence of specific inhibition of the BRBV RdRP is provided by failure of the flavonoid #201 to inhibit the endonuclease activity of B19V NS1 (Xu et al., 2018). Although compound #201 was cytotoxic at 10 μM in HEK293T cells, compounds #7, #9, and #315 were not (**Figure 6D**). The half maximal IC_{50} of compound #9 in the reporter system was 2.22 μM (**Figure 6E**). We next assayed the inhibitory effect of compound #9 on virus replication in both HEK293T and Vero cells. The half maximal EC_{50} of compound #9 against viral replication was 4.6 and 20.0 μM in HEK293T and Vero cells, respectively (**Figures 7A,B**). Notably, compound #9 had negligible 50% CC_{50} of 537 μM in HEK293T cells and >1 mM in Vero cells (**Figures 7C,D**).

Collectively, our results demonstrated that a parvoviral endonuclease activity inhibitor, compound #9 (myricetin), inhibits BRBV replication in cells through inhibition of the RdRP activity with a therapeutic index (TI = CC_{50}/EC_{50}) of >50.

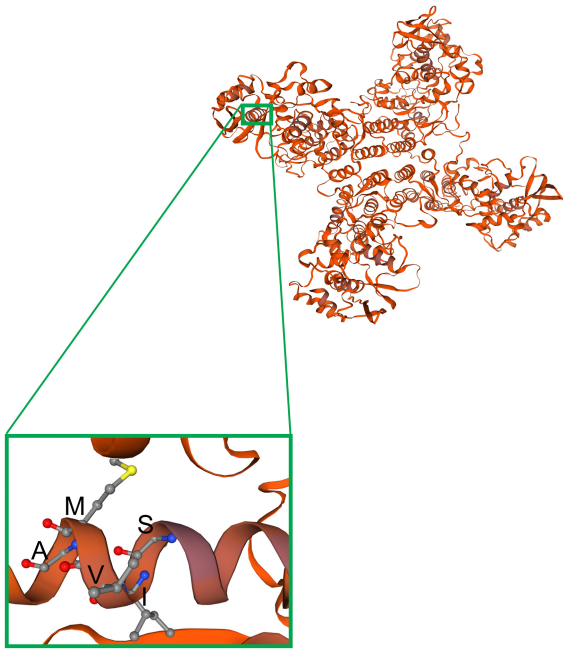

FIGURE 8 | Modeling of observed mutations in the a-helix structure of the NP protein. The BRBV NP structure was modeled on the template structure of the influenza D NP protein (Donchet et al., 2019) (SMTL ID: 5n2u.1) using SWISS-MODEL (Waterhouse et al., 2018). NP forms a tetramer, as shown, which has four arms and a center to capture viral RNA and pass it to the RdRP. The region of NP carrying the α-helix that includes aa 67-71 (SIVMA) is enlarged from one of the monomers.

DISCUSSION

In this study, we established a GFP/luciferase expression-based replicon reporter system for BRBV, and demonstrated it is suitable for screening of antivirals in a BSL2 setting. We identified myricetin (compound #9) as a potent anti-BRBV drug. As BRBV is classified a BSL3 agent, the replicon system of BRBV is important for screening antivirals in a high throughput format in a BSL2 setting. Our replicon reporter system of BRBV contains 4 plasmids, one in *cis* plasmid (pHW-ΔCMV-gLuc) and three in *trans* plasmids (pcDNA-PA, PB1, PB2, and NP). Transfection of all them into HEK293T cells results replication of the *gLuc* gene that is flanked with the 5′ and 3′ UTR of the BRBV GP genome. It will be ideal to integrate the pol I expression cassette (5′ UTR-gLuc-3′ UTR) and a CMV promoter expression cassette of PA-PB1-PB2-NP into one plasmid and use it in transfection, or to generate a cell line that hosts the replicon reporter, which is currently under construction.

In contrast to influenza viruses, thogotoviruses are transmitted mainly through tick vectors and thus are also called "tick-borne viruses" (Haig et al., 1965; Anderson and Casals, 1973). Phylogenetically, BRBV is most closely related to dhori virus and its subtype, batken virus, which have been known to occur in regions throughout Africa, Asia and Europe (Lvov et al., 1974; Moore et al., 1975; Filipe et al., 1985; Hubalek and Rudolf, 2012). Dhori and batken viruses have been isolated from *Hyalomma* ticks, and antibodies against dhori virus have been detected in camels, goats, horses, cattle, and humans (Lvov et al., 1974; Moore et al., 1975; Filipe et al., 1985; Hubalek and Rudolf, 2012). Interestingly, batken virus has also been isolated from several mosquito species (Lvov et al., 1974). BRBV replicates at a high level in a variety of invertebrate and vertebrate cell lines, including HEK293T cells, and produces relatively high titers in all mammalian cells that are compatible with the known susceptibility of the human host to BRBV infection and diseases (Lambert et al., 2015). However, it is possible that the lack of the endogenous expression of RIG-I (Fitzgerald et al., 2017), a key cytosolic RNA sensor, in HEK293T cells, or virus-expressed protein(s) that interrupt the innate immunity response in human cells, facilitates BRBV replication in HEK293 cells or human cells.

The cell cultured BRBV-KS has a series of sequence variations in one α-helix of the NP protein, compared to the originally reported sequences (KP657749) by direct sequencing of the patient's samples (**Figure 3B**). We modeled the structure of BRBV NP protein for the amino acids' electric charges and propensities to form an α-helix against the structure of influenza D virus (Donchet et al., 2019) using SWISS-MODEL (Waterhouse et al., 2018) (**Figure 8**). The modeling indicates that the variations at aa 67-71 did not change the charges of any amino acids, had minimal effects on the polarity of the variant sequences, and the sequence was still able to form an α-helix. Interestingly, the BRBV-STL strain, which was isolated from a fatal BRBV case in St. Louis,

MO, United States in 2017 (Bricker et al., 2019), had the identical sequence at aa 67-71 in the NP protein (MK453525) as that of the cell cultured BRBV-KS.

Currently, there is no treatment or vaccine for BRBV-infection caused diseases. Mice (CD-1) were susceptible to BRBV infection as evidenced by seroconversion, but the infection did not cause disease symptoms or death of the animals (Lambert et al., 2015). Recently, mice lacking IFN-α/β receptor expression (IFNαAR$^{-/-}$) have been used as an animal model to evaluate antivirals against BRBV (Bricker et al., 2019; Fuchs et al., 2019). Favipiravir, a pan inhibitor of RdRP (Furuta et al., 2005), was shown to protect IFNαAR$^{-/-}$ mice from lethal BRBV infection. The EC_{50} of favipiravir against BRBV infection of Vero was 310 μM (Bricker et al., 2019). In animals, administration of 150 mg/kg of favipiravir twice daily at 3 days post-infection protected all animals from death of BRBV infection. However, it was speculated that favipiravir reached a concentration of 1.28 mM in serum, leading to the argument that it is not practical to use favipiravir to treat BRBV-infected patients. Notably myricetin, that was identified in our study, has a 15-fold lower EC_{50} (20 μM) compared with the 310 μM of favipiravir in Vero cells, suggesting that myricetin may be a more potent inhibitor of BRBV infection than favipiravir. Due to the lack of an animal BSL3 facility that can host BRBV-infected IFNαAR$^{-/-}$ mice, we were not able to examine myricetin in animals.

Myricetin, a common plant-derived flavonoid, exhibits a wide range of activities, including antioxidant, anticancer, antidiabetic, and anti-inflammatory activities, as well as antimicrobial activities (Semwal et al., 2016). Myricetin was reported as a strong inhibitor of reverse transcriptase of retroviruses (Ono et al., 1990). It has also been shown to be active in inhibition of nsp13, a helicase of the severe acute respiratory syndrome (SARS) coronavirus helicase that targets the ATPase activity *in vitro* (IC_{50} = 2.71 μM) (Keum and Jeong, 2012; Yu et al., 2012). We found that myricetin does not exert obvious cytotoxicity in Vero and HEK239T cells, as well as in normal breast epithelial cells (Keum and Jeong, 2012; Yu et al., 2012). We previously found that myricetin inhibited over 90% of the endonuclease activity of B19V NS1N (the endonuclease domain of NS1) *in vitro* at 10 μM (Xu et al., 2018), and thus speculate that myricetin may inhibit the endonuclease activity of BRBV PA, which warrants further investigation.

DATA AVAILABILITY STATEMENT

The raw data supporting the conclusions of this article will be made available by the authors, without undue reservation.

AUTHOR CONTRIBUTIONS

JQ, JT, SH, and SG contributed to the conception of the study. SH, KN, XW, and FC performed the experiments. SH, KN, JW, and JQ analyzed the data. JQ, SH, and JT wrote the manuscript. All authors contributed to the article and approved the submitted version.

FUNDING

This study was supported by PHS grant AI144564 from the National Institute of Allergy and Infectious Diseases. The funders had no role in study design, data collection and interpretation, or the decision to submit the work for publication.

ACKNOWLEDGMENTS

We are grateful to Dr. Zekun Wang and other members of the Qiu Laboratory for technical support and valuable discussions. We thank Dr. Wenjun Ma at Kansas State University for providing the pHW2000 plasmid. The following reagent was obtained through BEI Resources, NIAID, NIH: Bourbon Virus, Original, NR-50132.

SUPPLEMENTARY MATERIAL

The Supplementary Material for this article can be found online at: https://www.frontiersin.org/articles/10.3389/fmicb.2020.572631/full#supplementary-material

REFERENCES

Anderson, C. R., and Casals, J. (1973). Dhori virus, a new agent isolated from Hyalomma dromedarii in India. *Indian J. Med. Res.* 61, 1416–1420.

Bricker, T. L., Shafiuddin, M., Gounder, A. P., Janowski, A. B., Zhao, G., Williams, G. D., et al. (2019). Therapeutic efficacy of favipiravir against Bourbon virus in mice. *PLoS Pathog.* 15:e1007790. doi: 10.1371/journal.ppat.1007790

Butenko, A. M., Leshchinskaia, E. V., Semashko, I. V., Donets, M. A., and Mart'ianova, L. I. (1987). [Dhori virus–a causative agent of human disease. 5 cases of laboratory infection]. *Vopr. Virusol.* 32, 724–729.

Byrn, R. A., Jones, S. M., Bennett, H. B., Bral, C., Clark, M. P., Jacobs, M. D., et al. (2015). Preclinical activity of VX-787, a first-in-class, orally bioavailable inhibitor of the influenza virus polymerase PB2 subunit. *Antimicrob. Agents Chemother.* 59, 1569–1582. doi: 10.1128/aac.04623-14

Dias, A., Bouvier, D., Crepin, T., McCarthy, A. A., Hart, D. J., Baudin, F., et al. (2009). The cap-snatching endonuclease of influenza virus polymerase resides in the PA subunit. *Nature* 458, 914–918. doi: 10.1038/nature07745

Doan, L., Handa, B., Roberts, N. A., and Klumpp, K. (1999). Metal ion catalysis of RNA cleavage by the influenza virus endonuclease. *Biochemistry* 38, 5612–5619. doi: 10.1021/bi9828932

Donchet, A., Oliva, J., Labaronne, A., Tengo, L., Miloudi, M., Gerard, C. A., et al. (2019). The structure of the nucleoprotein of Influenza D shows that all Orthomyxoviridae nucleoproteins have a similar NPCORE, with or without a NPTAIL for nuclear transport. *Sci. Rep.* 9:600.

Filipe, A. R., Calisher, C. H., and Lazuick, J. (1985). Antibodies to Congo-Crimean haemorrhagic fever, Dhori, Thogoto and Bhanja viruses in southern Portugal. *Acta Virol.* 29, 324–328.

Fitzgerald, M. E., Rawling, D. C., Potapova, O., Ren, X., Kohlway, A., and Pyle, A. M. (2017). Selective RNA targeting and regulated signaling by RIG-I is

controlled by coordination of RNA and ATP binding. *Nucleic Acids Res.* 45, 1442–1454.

Fuchs, J., Straub, T., Seidl, M., and Kochs, G. (2019). Essential role of interferon response in containing human pathogenic bourbon virus. *Emerg. Infect. Dis.* 25, 1304–1313. doi: 10.3201/eid2507.181062

Furuta, Y., Komeno, T., and Nakamura, T. (2017). Favipiravir (T-705), a broad spectrum inhibitor of viral RNA polymerase. *Proc. Jpn. Acad. Ser. B Phys. Biol. Sci.* 93, 449–463. doi: 10.2183/pjab.93.027

Furuta, Y., Takahashi, K., Kuno-Maekawa, M., Sangawa, H., Uehara, S., Kozaki, K., et al. (2005). Mechanism of action of T-705 against influenza virus. *Antimicrob. Agents Chemother.* 49, 981–986. doi: 10.1128/aac.49.3.981-986.2005

Haig, D. A., Woodall, J. P., and Danskin, D. (1965). Thogoto virus: a hitherto underscribed agent isolated from tocks in kenya. *J. Gen. Microbiol.* 38, 389–394. doi: 10.1099/00221287-38-3-389

Hoffmann, E., Mahmood, K., Yang, C. F., Webster, R. G., Greenberg, H. B., and Kemble, G. (2002). Rescue of influenza B virus from eight plasmids. *Proc. Natl. Acad. Sci. U.S.A.* 99, 11411–11416. doi: 10.1073/pnas.172393399

Hubalek, Z., and Rudolf, I. (2012). Tick-borne viruses in Europe. *Parasitol. Res.* 111, 9–36. doi: 10.1007/s00436-012-2910-1

Jackson, K. C., Gidlewski, T., Root, J. J., Bosco-Lauth, A. M., Lash, R. R., Harmon, J. R., et al. (2019). Bourbon Virus in Wild and Domestic Animals, Missouri, USA, 2012-2013. *Emerg. Infect. Dis.* 25, 1752–1753. doi: 10.3201/eid2509.181902

Kawaoka, Y., and Palese, P. (2006). "Family Orthomyxoviridae," in *Virus Taxonomy: Eighth Report of the International Committee on Taxonomy of Viruses*, eds C. M. Fauquet, M. A. Mayo, J. Maniloff, U. Desselberger, and L. Ball (San Diego, CA: Academic Press), 681–693.

Keum, Y. S., and Jeong, Y. J. (2012). Development of chemical inhibitors of the SARS coronavirus: viral helicase as a potential target. *Biochem. Pharmacol.* 84, 1351–1358. doi: 10.1016/j.bcp.2012.08.012

Klumpp, K., Doan, L., Roberts, N. A., and Handa, B. (2000). RNA and DNA hydrolysis are catalyzed by the influenza virus endonuclease. *J. Biol. Chem.* 275, 6181–6188. doi: 10.1074/jbc.275.9.6181

Kosoy, O. I., Lambert, A. J., Hawkinson, D. J., Pastula, D. M., Goldsmith, C. S., Hunt, D. C., et al. (2015). Novel thogotovirus associated with febrile illness and death, United States, 2014. *Emerg. Infect. Dis.* 21, 760–764.

Lambert, A. J., Velez, J. O., Brault, A. C., Calvert, A. E., Bell-Sakyi, L., Bosco-Lauth, A. M., et al. (2015). Molecular, serological and in vitro culture-based characterization of Bourbon virus, a newly described human pathogen of the genus Thogotovirus. *J. Clin. Virol.* 73, 127–132. doi: 10.1016/j.jcv.2015.10.021

Lvov, D. K., Karas, F. R., Tsyrkin, Y. M., Vargina, S. G., Timofeev, E. M., Osipova, N. Z., et al. (1974). Batken virus, a new arbovirus isolated from ticks and mosquitoes in Kirghiz S.S.R. *Arch. Gesamte Virusforsch.* 44, 70–73. doi: 10.1007/bf01242183

Moore, D. L., Causey, O. R., Carey, D. E., Reddy, S., Cooke, A. R., Akinkugbe, F. M., et al. (1975). Arthropod-borne viral infections of man in Nigeria, 1964-1970. *Ann. Trop. Med. Parasitol.* 69, 49–64. doi: 10.1080/00034983.1975.11686983

Omoto, S., Speranzini, V., Hashimoto, T., Noshi, T., Yamaguchi, H., Kawai, M., et al. (2018). Characterization of influenza virus variants induced by treatment with the endonuclease inhibitor baloxavir marboxil. *Sci. Rep.* 8:9633.

Ono, K., Nakane, H., Fukushima, M., Chermann, J. C., and Barre-Sinoussi, F. (1990). Differential inhibitory effects of various flavonoids on the activities of reverse transcriptase and cellular DNA and RNA polymerases. *Eur. J. Biochem.* 190, 469–476. doi: 10.1111/j.1432-1033.1990.tb15597.x

Savage, H. M., Burkhalter, K. L., Godsey, M. S. Jr., Panella, N. A., Ashley, D. C., Nicholson, W. L., et al. (2017). Bourbon virus in field-collected ticks, Missouri, USA. *Emerg. Infect. Dis.* 23, 2017–2022. doi: 10.3201/eid2312.170532

Savage, H. M., Godsey, M. S. Jr., Panella, N. A., Burkhalter, K. L., Manford, J., Trevino-Garrison, I. C., et al. (2018). Surveillance for Tick-Borne Viruses Near the Location of a Fatal Human Case of Bourbon Virus (Family Orthomyxoviridae: genus Thogotovirus) in Eastern Kansas, 2015. *J. Med. Entomol.* 55, 701–705. doi: 10.1093/jme/tjx251

Semwal, D. K., Semwal, R. B., Combrinck, S., and Viljoen, A. (2016). Myricetin: a dietary molecule with diverse biological activities. *Nutrients* 8:90. doi: 10.3390/nu8020090

Sun, Y., Chen, A. Y., Cheng, F., Guan, W., Johnson, F. B., and Qiu, J. (2009). Molecular characterization of infectious clones of the minute virus of canines reveals unique features of bocaviruses. *J. Virol.* 83, 3956–3967. doi: 10.1128/jvi.02569-08

Wang, Z., Cheng, F., Engelhardt, J. F., Yan, Z., and Qiu, J. (2018). Development of a Novel Recombinant Adeno-Associated Virus Production System Using Human Bocavirus 1 Helper Genes. *Mol. Ther. Methods Clin. Dev.* 11, 40–51. doi: 10.1016/j.omtm.2018.09.005

Waterhouse, A., Bertoni, M., Bienert, S., Studer, G., Tauriello, G., Gumienny, R., et al. (2018). SWISS-MODEL: homology modelling of protein structures and complexes. *Nucleic Acids Res.* 46, W296–W303.

Xu, P., Ganaie, S. S., Wang, X., Wang, Z., Kleiboeker, S., Horton, N. C., et al. (2018). Endonuclease activity inhibtion of the NS1 protein of parvovirus B19 as a novel target for antiviral drug developemnt. *Antimicrob. Agents Chemother.* 63:e1879-18.

Yu, M. S., Lee, J., Lee, J. M., Kim, Y., Chin, Y. W., Jee, J. G., et al. (2012). Identification of myricetin and scutellarein as novel chemical inhibitors of the SARS coronavirus helicase, nsP13. *Bioorg. Med. Chem. Lett.* 22, 4049–4054. doi: 10.1016/j.bmcl.2012.04.081

Conflict of Interest: The authors declare that the research was conducted in the absence of any commercial or financial relationships that could be construed as a potential conflict of interest.